Am J Transl Res 2015;7(8):1404-1416
www.ajtr.org /ISSN:1943-8141/AJTR0011680

Original Article

Protective effects of perfluorooctyl-bromide nanoparticles on early brain injuries following subarachnoid hemorrhage in rats

Huan Zhang[1], Rui Xu[1], Fei Xie[1], Wei Xu[1], Meng-Fei Zeng[1], Xin Wang[2], Ji Zhu[1]

[1]Department of Neurosurgery, The First Affiliated Hospital of Chongqing Medical University, Chongqing 400016, China; [2]Department of Neurosurgery, Brigham and Women's Hospital, Harvard Medical School, Boston, Massachusetts 02115, USA

Received June 20, 2015; Accepted July 31, 2015; Epub August 15, 2015; Published August 30, 2015

Abstract: To investigate the protective effects of perfluorooctyl-bromide (PFOB) nanoparticles on early brain injury (EBI) following subarachnoid hemorrhage (SAH), a total of 120 rats were randomly assigned to the following groups: Sham operation group (n = 40), SAH group (n = 40), and SAH + PFOB group (n = 40). Endovascular perforation was performed to induce subarachnoid hemorrhage. Brain water content was measured 24 h after surgery. Meanwhile, morphological changes in the rat hippocampal CA1 region were examined using light and transmission electron microscopy. The rate of neuronal apoptosis in rat hippocampal CA1 region was determined using TUNEL assay. Protein and mRNA expression levels of Caspase-3, Bax, and Bcl-2 were measured using western blot and RT-PCR assays 12, 24, 48, and 72 h after surgery. Compared to the SAH group, the SAH + PFOB group had significantly lower brain water content ($P<0.01$), with alleviated morphological abnormalities in HE-stained neurons and significantly decreased neurons with karyopyknosis and hyperchromatism in the hippocampal CA1 region. Electron microscopy revealed reduction of neuronal apoptosis, alleviation of glial cell swelling, and mitigation of perivascular edema in the hippocampal region. Immunohistochemical analysis showed that the expression of apoptosis-related factors Caspase-3 and Bax was significantly reduced, while that of the anti-apoptotic factor Bcl-2 was significantly increased. TUNEL staining showed that neuronal apoptosis was significantly reduced in the hippocampal CA1 region ($P<0.01$). RT-PCR and Western-blot data indicated that expressions of Caspase-3 and Bax were both significantly reduced, while bcl-2 expression was increased significantly at 12, 24, 48, and 72 h after SAH ($P<0.01$). Together, our data support that PFOB nanoparticles with high oxygen content could counteract ischemia and hypoxia, block neuronal apoptotic pathways, reduce neuronal apoptosis, and therefore, achieve neuroprotective effects in EBI following SAH.

Keywords: Subarachnoid hemorrhage, perfluorooctyl-bromide, early brain injury, neuroprotection, apoptosis

Introduction

Subarachnoid Hemorrhage (SAH) is a form of acute stroke with high mortality and disability rates [1]. With the aging of the population, changes in dietary habits, and improvements in diagnosis, the number of SAH patients will increase. Therefore, emphasis on the prevention and treatment of SAH is urgently needed. Once SAH occurs, the blood that quickly flows out of the cistern or the ventricle sharply raises intracranial pressure, followed by the reduction in cerebral perfusion, resulting in brain-wide ischemia and hypoxia, while inducing a variety of stress responses through a number of signal transduction pathways. These form the pathological changes after SAH onset. Therefore, the series of pathological changes within 72 hours after SAH onset is known as early brain injury (EBI) [2-4]. The main components of EBI are currently considered to include brain-wide ischemia, damage to the blood-brain barrier, brain edema, immunological inflammation and cell apoptosis, following SAH [5-7].

Perfluorooctyl-bromide (PFOB) is a new-generation perfluorocarbon (PFC). It is widely used in research on contrast agents for ultrasound, CT and MR due to its characteristic blockage of radiation, acoustic and magnetic properties, as

well as its safety and stability [8]. At the same time, because PFOB has very high oxygen-carrying capacity, good diffusibility, low surface tension, low viscosity, high density, and high gas solubility [9-11], it has also been widely used in many biomedical areas. However, the effect of PFC on SAH has not been reported. In this study, we employed high-oxygen-concentration PFOB nanoparticle intervention in the rat SAH model and demonstrated that PFOB is protective against EBI following SAH.

Materials and methods

Reagents

PFOB was obtained from Alliance Pharmaceutical, USA. It was made into emulsified nanoparticles that were 90.2 ± 8.3 nm in diameter by the Ultrasound Imaging Institute, Chongqing University of Medical Science. Immunohistochemistry kits were purchased from BioWorld, USA. TUNEL kits were purchased from Roche; DAB developing solution was from DAKO; Trizol kit was purchased from Invitrogen; and the cDNA reverse-transcription reagent kit purchased from Fermant. Bax, Bcl-2 antibody was purchased from Santa; and Caspase-3 antibody from Abcam. The primers were designed and composed by Songon Biotech, Shang Hai, China. The other reagents were provided by First Affiliated Hospital of Chongqing Medical University Experiment Center.

Ethics statement

All procedures were approved by the Institutional Animal Care Committee of Chongqing Medical University and were performed in accordance with the guidelines of the National Institutes of Health on the care and use of animals.

Animals and grouping

Adult healthy male SD rats weighing 300 ± 5 g were provided by the Experimental Animal Center of Chongqing Medical University. All rats were grown in a standard environment (12 h of light/dark cycle, temperature 22 ± 1 and humidity 55 ± 5%) and given free of food and water intake. They were divided into three groups: Sham group, SAH group and SAH + PFOB group. SAH was performed by endovascular perforation with 4 to 0nylon monofilament sutures [12]. The SAH + PFOB group was injected with PFOB Nano-emulsification (5 g/kg) with high oxygen concentration through the tail vein three hours after successfully producing the model. Chloral hydrate (10%, 300 mg/kg) was injected intraperitoneally for anesthesia. During the operation, a heat unit was used to maintain body temperature, and breathing and heart rate were monitored.

Brain water content measurement

The rats from each group were selected and sacrificed by decapitation 24 h after the operation. Brain tissue was removed and weighed immediately (using the dry-wet method) before being dried in an oven until the weight became constant. The brain water content was calculated using the follow formula: Brain tissue water content (%) = (wet weight-dry weight)/wet weight × 100% as previously described [13].

Hematoxylin and eosin (HE) staining

All groups were injected with 4% paraformaldehyde 24 h after producing the model, and their brains were taken to create specimens. Paraffin sections of rat brain tissues were made, which underwent dewaxing, hematoxylin staining, acid and ammonia washes, running water wash, alcohol dehydration, eosin staining, dehydration, neutral gum mounting, and observation.

Transmission electron microscopy

Twenty-four hours after model establishment and PFOB intervention, 4% of glutaraldehyde was administered to the brain tissue. Samples of CA1 region for electron microscopy were fixed in phosphate-buffered glutaradehyde (2.5%) and osmium tetroxide (1%). Dehydration of the cortex was accomplished in acetone solutions at increasing concentrations. The tissue was embedded in an epoxy resin. Semi-thin (1 μm) sections through the sample were then made and stained with toluidine blue. Then, 600-Å sections were made from a selected area of tissue defined by the semi-thin section, and these sections were stained with lead citrate and uranyl acetate. The ultrastructure of the brain was observed under a transmission electron microscope (JEM-1010).

Immunohistochemistry

Twenty-four hours after model establishment and PFOB intervention, brain tissue specimens were collected. The ABC method was used for immunohistochemical reactions. The sections were dewaxed using xlyene and an alcohol gradient placed in 3% peroxide and incubated for 30 min to stop the activity of the endogenous catalase. Sections were then washed three times with 0.01 mol/L PBS for 5 min each time. The antigens were heat-revived, and the sections were incubated in normal goat serum working solution at 37°C for 30 min. The normal goat serum was discarded, and the rabbit-anti-Caspase-3 polyclonal antibody (working concentration 1:250), rabbit-anti-Bcl-2 (1:300), rabbit-anti-Bax (1:300) was added to the sections and incubated overnight at 4°C. The sections were washed three times with 0.01 mol/L PBS for 5 min each and incubated with horseradish peroxide (HRP)-labeled active rabbit-anti-goat IgG working solution at 37°C for 30 min and washed three times with 0.01 mol/L PBS for 5 min each time. The sections were then stained for 3-5 min in DAB staining solution, restained in hematoxylin, differentiated using hydrochloric alcohol, and gradient dehydrated. After the sections were sealed with neutral balsam, photos were taken and analyzed.

Terminal deoxynucleotidyltransferase-mediated dUTP nick end labeling assay (TUNEL)

24 h after model establishment, brain tissue specimens perfused with 4% paraformaldehyde were collected and used as specimens. Paraffin-embedded sections of CA1 region were made, and underwent dewaxing, membrane rupture recovery by antigen, endogenous peroxidase activity blocking, DAB staining, restaining, hydrochloric acid alcohol differentiation, counterstaining, and dehydration as previously described [14]. Their pictures were taken and analyzed after being mounted with neutral gum.

RT-PCR

The total RNA in each sample mentioned was extracted using the TRIzol reagent kit. The primers were designed according to rat Caspase-3, Bax, and Bcl-2cDNA sequence. Caspase-3: upstream: 5-GCCGACTTCCTGTATGCT-3, downstream: 5-GGACTAAATTCCGTGGC-3; The amplification product was 177 bp long. Bax: upstream: 5-GCAAACTGGTGCTCAAGG-3, downstream: 5-GACTCCAGCACAAAGATG-3. The amplification product was 188 bp long. Bcl-2: upstream: 5-GGAGCGTCAACAGGGAGA-3, downstream 5-AGACAGCCAGGAGAAATCAA-3. The amplification product was 170 bp long. GAPDH was used as an internal control with its primers as: upstream:5-GTTCAACGGCACAGTCAA-3, downstream:5-CTCGCTCCTGGAAGATGG-3; The amplification product was 77 bp long. Equal amounts (1 μg) of total RNA were taken from each of the samples mentioned above and cNDA was produced using the AMV reverse-transcription reagent kit. One μL of each of the resultant cDNA was used as a template in PCR reactions together with primers mentioned above (the volume of the reaction was 25 μL). PCR amplification conditions were 95°C predenaturation for 1 min, 95°C for 15 s, 58°C for 15 s, and 72°C for 45 s, repeated for 40 cycles. To analyze the result, 5 μL of the PCR product was subjected to agarose gel electrophoresis. The result was recorded using a UV gel imaging analysis system. ImageJ software was used to measure the average grayscale and area of each electrophoresis band.

Western blot analysis

Five rats were randomly selected from each group. Their brains were extracted, placed in cell lysis buffer, and homogenized at low temperature. They were then left standing for 10 min and 90 μL of 100 g/L NP-40 was added. They were shaken vigorously for 30 seconds and centrifuged at 4°C, 13000 rpm for 15 min. The supernatant was removed and stored separately at -80°C. Using protein quantification, electrophoresis, electric transfer, hybridization and detection, quantitative analysis was performed for Caspase-3, Bax, and Bcl-2 protein. Optical density scanning was performed on each sample strip to determine and statistically analyze the optical density value of each group.

Statistical analysis

SPSS statistical software was used for analysis; normal-distribution data were presented as mean ± standard deviation ($x \pm s$). The experimental groups were compared using one-way ANOVA, and inter-group paired comparisons were examined by LSD.

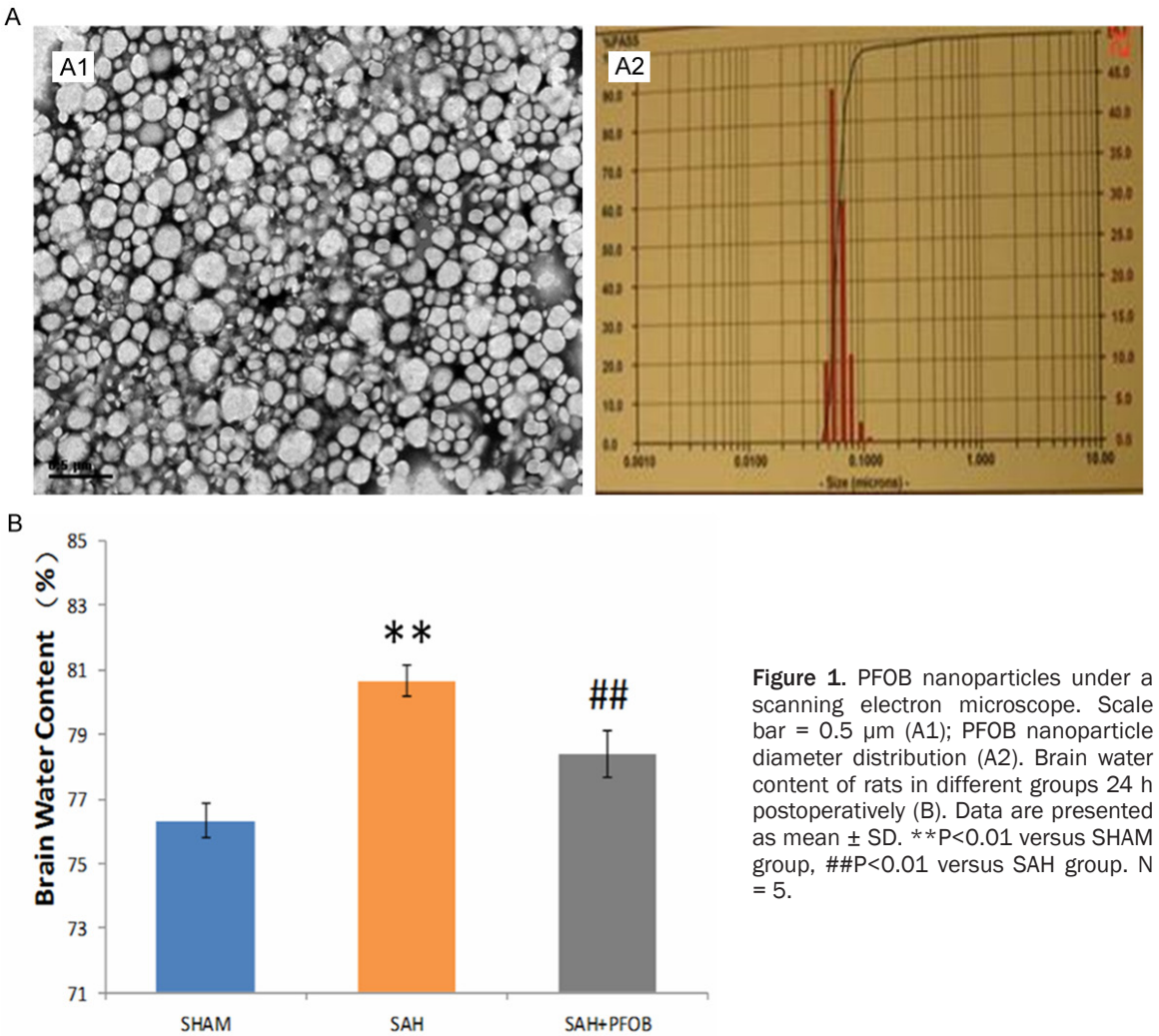

Figure 1. PFOB nanoparticles under a scanning electron microscope. Scale bar = 0.5 μm (A1); PFOB nanoparticle diameter distribution (A2). Brain water content of rats in different groups 24 h postoperatively (B). Data are presented as mean ± SD. **P<0.01 versus SHAM group, ##P<0.01 versus SAH group. N = 5.

Results

Production of PFOB emulsification nanoparticles

The appearance of PFOB nanoparticles was an even emulsion, which did not stratify after standing for over one hour at room temperature. It could remain stable for over one month in a 4°C fridge, with no obvious change in appearance or form when observed using the naked eye or a microscope. PFOB nanoparticles (**Figure 1A**) were fine and dense, with a regular shape and a spherical distribution. There was no obvious accumulation. The diameters of PFOB nanoparticles were 90.2 ± 8.3 nm (**Figure 1A**), with an average of 90.2 nm and a narrow distribution. The nanoparticle surface electric potential was 9.5 ± 3.1 mV, with an average of 12.3 mV. The particle arrangement in this nano-level PFOB emulsification is close to capillary wall and can cross blood vessel walls and brain tissues easily, thus greatly reducing the distance of oxygen transportation.

PFOB significantly reduces the brain water content in animal model of SAH

As reported PFCs plays a protection role after animal cerebral stroke [15], recovery of consciousness after craniocerebral trauma [16], and protection of neurons after spinal cord injury [17]. However, the effect of PFC, in particularly, the effect of PFOB, the third generation of PFCs, on SAH has not been reported. We therefore investigated the effect of PFOB on SAH by measuring the brain water content 24 h after surgery. As in **Figure 1B**, the SAH group had substantially increased brain water con-

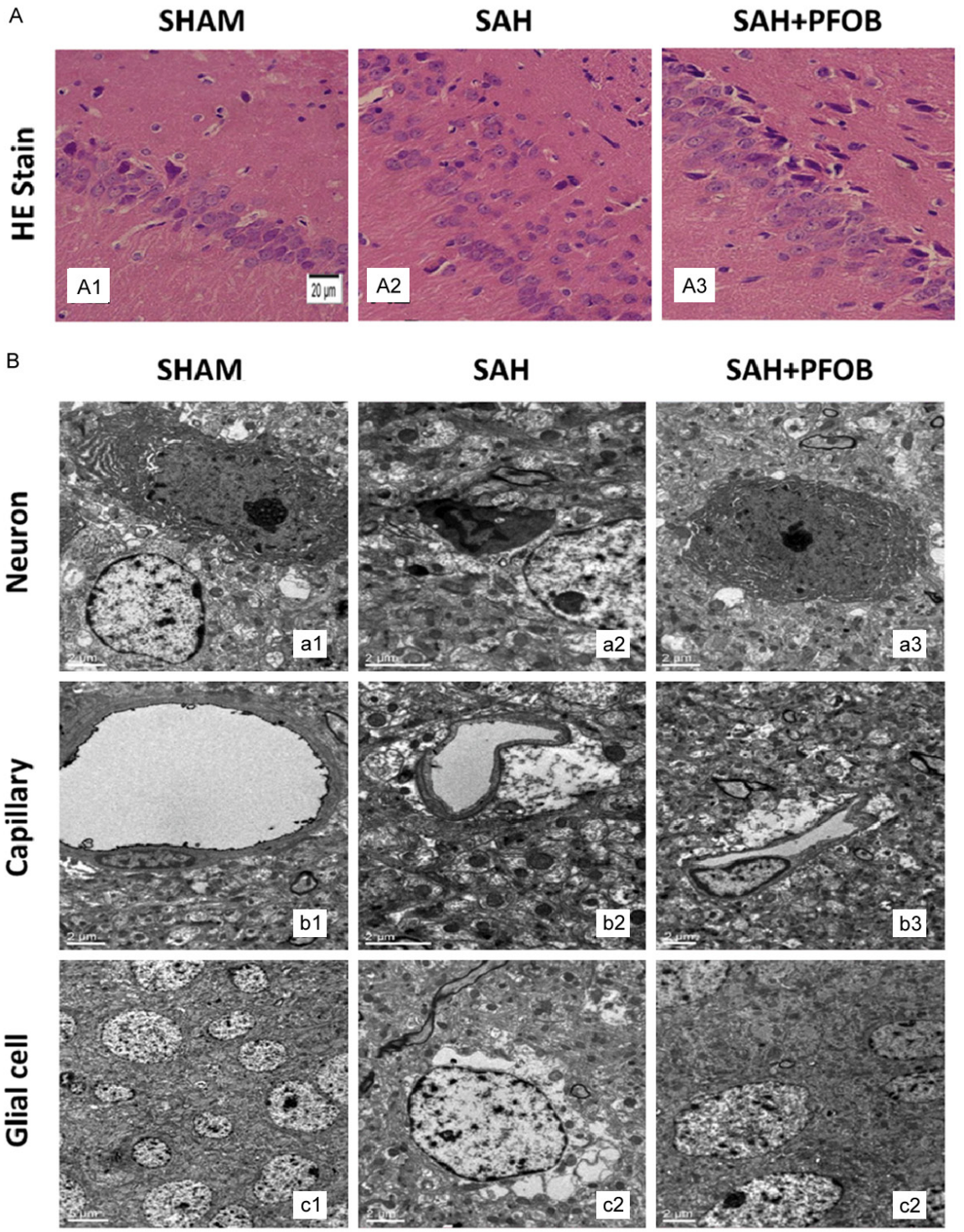

Figure 2. HE stain of Hippocampus CA1 region (A). SHAM group, normalneural morphology (A1); SAH group, neurons showed cytoplasmic condensation, hyperchromatism and karyopyknosis (A2); PFOB intervention group (A3). Scale bar = 20 μm. N = 5. Transmission electron microscopy examination (B). N = 5.

tent compared to the SHAM group (80.65 ± 0.49 vs 76.32 ± 0.52; $p<0.01$). On the other hand, there was a statistically significant reduction in brain water content in the SAH + PFOB

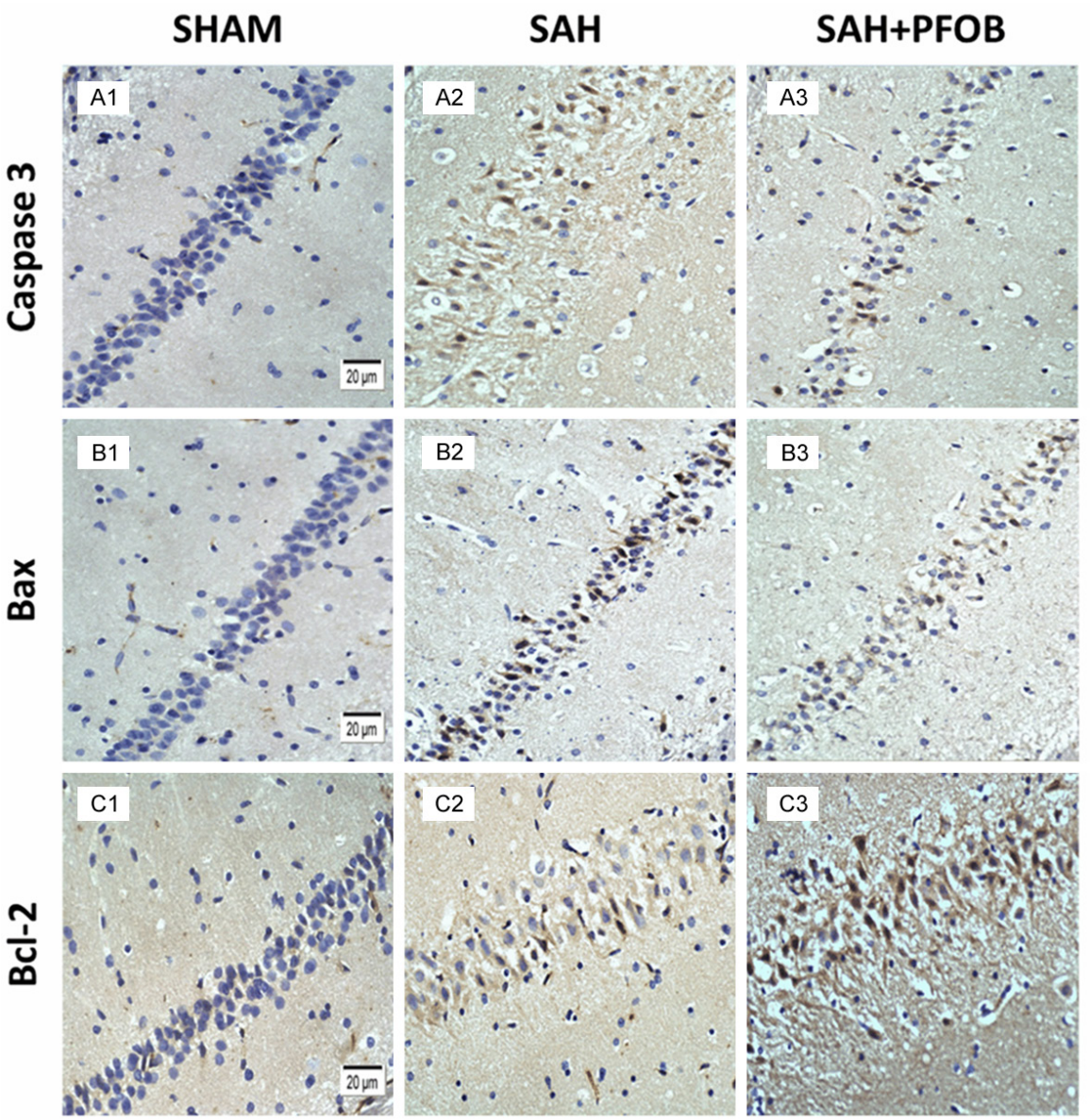

Figure 3. Immunohistochemical analysis of caspase-3, Bax and Bcl-2 expressions in the hippocampal CA1 region. A1-A3 showed caspase-3 expression in the SHAM, SAH, and SAH + PFOB groups, respectively; B1-B3 represent bax expression in the SHAM, SAH, and SAH + PFOB groups, respectively; and C1-C3 represent bcl-2 expression in the SHAM, SAH, and SAH + PFOB groups, respectively. Scale Bar = 20 μm. N = 5.

group compared to the SAH group (78.40 ± 0.72 vs 80.65 ± 0.49; $p<0.01$).

Light and transmission electron microscopy of Hippocampus CA1 region

The hippocampus is an important part of the limbic system, an area of the brain playing a central role in stress responses. Hippocampal neurons are the most sensitive to ischemia and hypoxia, and the most vulnerable to ischemia and hypoxia injury. The number of delayed cell death among pyramidal cells is often used as a sign of cerebral ischemic injury severity. Meanwhile hippocampal tissues are easily to separated and identify. Thus, in the study, we chose hippocampal neurons as our target, and Caspase-3, Bax, and Bcl-2 as the studying molecules to study.

The hippocampus CA1 region was HE stained and subjected to 400X light microscopy. IN the SHAM group, the hippocampus CA1 region neurons showed normal morphology; the neurons

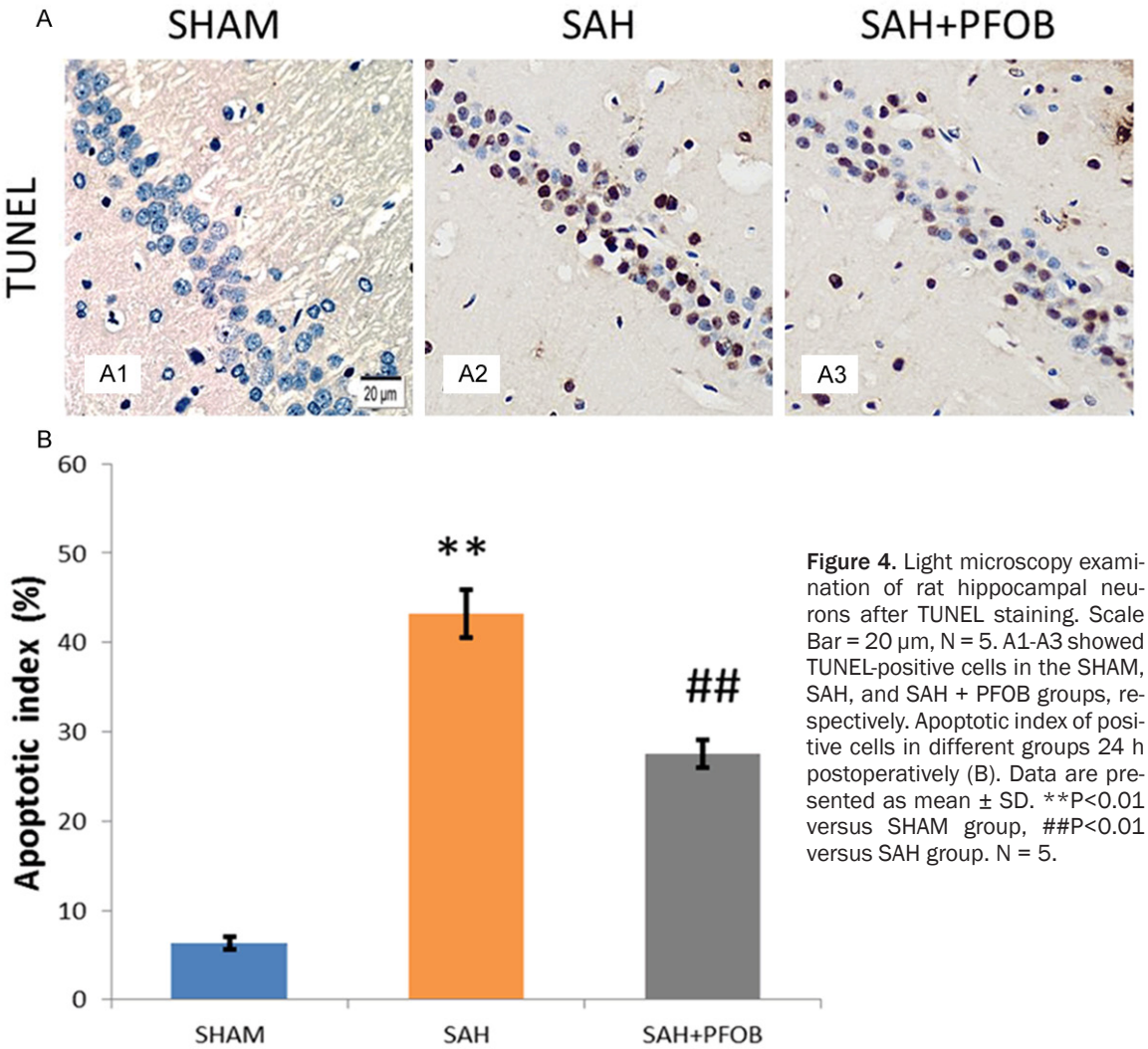

Figure 4. Light microscopy examination of rat hippocampal neurons after TUNEL staining. Scale Bar = 20 μm, N = 5. A1-A3 showed TUNEL-positive cells in the SHAM, SAH, and SAH + PFOB groups, respectively. Apoptotic index of positive cells in different groups 24 h postoperatively (B). Data are presented as mean ± SD. **P<0.01 versus SHAM group, ##P<0.01 versus SAH group. N = 5.

in the CA1 region of the SAH group showed cytoplasmic condensation, hyperchromatism, and karyopyknosis; the CA1 region of the SAH + PFOB group showed reduced abnormal neural morphology and fewer karyopyknotic and/or hyperchromatic neurons (**Figure 2A**).

CA1 region was examined by transmission electron microscopy. In the SAH group, shrinkage of neuronal cells was observed, with karyopyknosis, hyperchromatism, and cytoplasmic hyperchromatin. Also, glial cells were swollen and dissolved, accompanied by chromatin margination and nuclear swelling. Perivascular edema of capillary vessels was obvious. In the SAH + PFOB group, neuronal apoptosis and the abovementioned morphological changes were not found. There was only slight expansion of the neuronal endoplasmic reticulum and mild swelling of mitochondria. In the SHAM group, normal morphology of cells was observed without any of the changes mentioned above (**Figure 2B**).

PFOB inhibits the activation of caspase-3, the number of TUNEL-positive cells, and the expressions of Bax and Bcl-2 in the hippocampal CA1 region

Caspase-3 is one of the major effectors in apoptosis, and the point of convergence in the transduction of a variety of apoptotic stimuli signals and has been frequently used as an indicator in studies on apoptosis [18]. Research has shown that Bcl-2 and Bax protein levels are directly related to the regulation of apoptosis: increased Bax promotes apoptosis [19], while increased Bcl-2 inhibits apoptosis [20]. Neuroprotection in this in vivo animal model of stroke is associated with inhibition caspase-3 activation [21-23] and Bax, and enhancement of

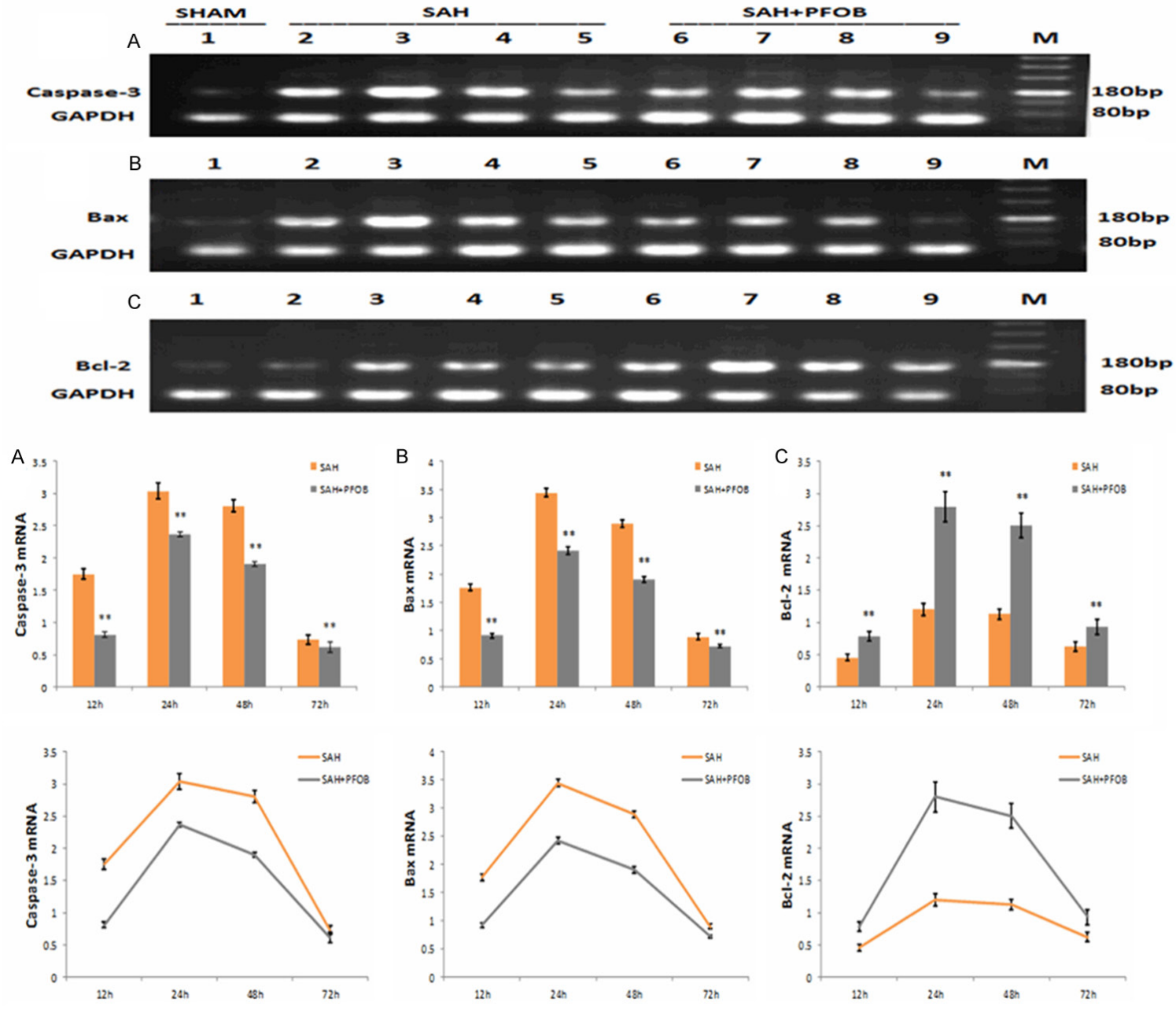
SHAM
SAH
SAH+PFOB
A
1 2 3 4 5 6 7 8 9 M
Caspase-3
GAPDH
180bp
80bp
B
1 2 3 4 5 6 7 8 9 M
Bax
GAPDH
180bp
80bp
C
1 2 3 4 5 6 7 8 9 M
Bcl-2
GAPDH
180bp
80bp
A
B
C
SAH
SAH+PFOB
Caspase-3 mRNA
Bax mRNA
Bcl-2 mRNA
12h
24h
48h
72h

Figure 5. RT-PCR measurement of caspase-3, Bax, and Bcl-2 mRNA expression. 1: the SHAM group; 2-5: the SAH group at 12, 24, 48, and 72 hours postoperatively; 6-9: the SAH + PFOB group at 12, 24, 48, and 72 hours postoperatively; and M: marker. Data are presented as mean ± SD. **P<0.01 versus SAH group (12 h; 24 h; 48 h; 72 h). N = 5.

Bcl-2 [24]. We next investigate whether PFOB inhibits the activation of Caspase-3 and the expression of Bax, and increases the expression of Bcl-2. In the SHAM group, we found there was no expression of Caspase-3, Bax, or Bcl-2 protein was observed, while in the SAH group we noted increased expression of all three proteins. Compared to the SAH group, the SAH + PFOB group had significantly reduced Caspase-3 and Bax expressions but increased Bcl-2 expression (**Figure 3**).

Neurons in the hippocampal CA1 regions of rats were examined by light microscopy at 400× magnification. A small amount of TUNEL-positive cells were observed in the SHAM group, while the SAH group had significantly increased number of TUNEL-positive cells (43.23 ± 2.67 vs 6.33 ± 0.72; P<0.01). In the SAH + PFOB group, expression of TUNEL-positive cells was significantly lower than in the SAH group (27.48 ± 1.53 vs 43.23 ± 2.67; P< 0. 01) (**Figure 4A** and **4B**).

After successful model establishment and drug intervention, hippocampal tissue specimens were collected, and total RNA was extracted from the tissue homogenates for RT-PCR analysis. Results showed that compared to the SAH group, the SAH + PFOB group had significantly lower expression of Caspase-3 mRNA (P<0.01 at 12, 24, 48 and 72 hours postoperatively) and Bax (P<0.01) at different time points, whereas Bcl-2 mRNA expression in the group increased significantly at different time points (P<0.01) (**Figure 5**).

Hippocampal protein was extracted for Western Blot analysis at 12, 24, 48, and 72 hours after successful model establishment and drug intervention. Compared to the SAH group, the SAH + PFOB group had significantly lower Caspase-3 and Bax protein expression (P<0.01) and increased Bcl-2 expression at different time points (P<0.01) (**Figure 6**).

Discussions

SAH has acute onset and an incidence of around 2-22.5 cases/100,000 people, thus affecting a large population. Once SAH occurs, EBI and delayed cerebral vasospasm can cause severe damage and might even lead to death. Due to our lack of understanding of this illness, limited surgical conditions for hospitals to carry out emergency examination and operations, the secondary impact of early-stage surgery on the patients, unmet surgery requirements in the early stage of the illness when the brain injury is too serious, and other factors, the majority of the patients cannot receive effective treatment in the early stage of SAH onset. Therefore, the features of SAH include rapid onset, high rates of disability or death, difficult of early treatment, and so on. Thus some researchers promoted the concept of EBI following SAH, which mainly consists of a series of pathological changes, including brain-wide ischemia, damage to the blood-brain barrier, brain edema, immunological inflammation, and cell apoptosis within 72 h after SAH, which are the factors most responsible for early-stage mortality and disability in SAH patients.

Complications of SAH include global cerebral ischemia, cerebral edema, oxidative stress responses, and immune inflammatory reactions, which can cause extensive apoptosis [25-26].

PFCs are a group of compounds with a wide range of biomedical applications [27]. Fluorine substituents gives the fluorocarbon molecules special features, such as thermal, chemical, and biological inertness; impermeability to radiation; good diffusibility; low surface tension; low viscosity; high density; and high gas solubility, all of which are the basis for innovative applications of PFCs. Since the pioneering work of Clark et al [28] in developing PFCs as respiratory gas carriers, PFCs have been used in multiple fields such as blood substitutes [29], liquid ventilation treatment of respiratory diseases [30], coronary angioplasty for myocardial infarction in the cardiovascular system, emergency treatment of carbon dioxide poisoning, targeted drug carriers [31], and new contrast agents [32]. In the field of neurosurgery, several applications of PFC have been revealed, including increasing cerebral blood flow, scav-

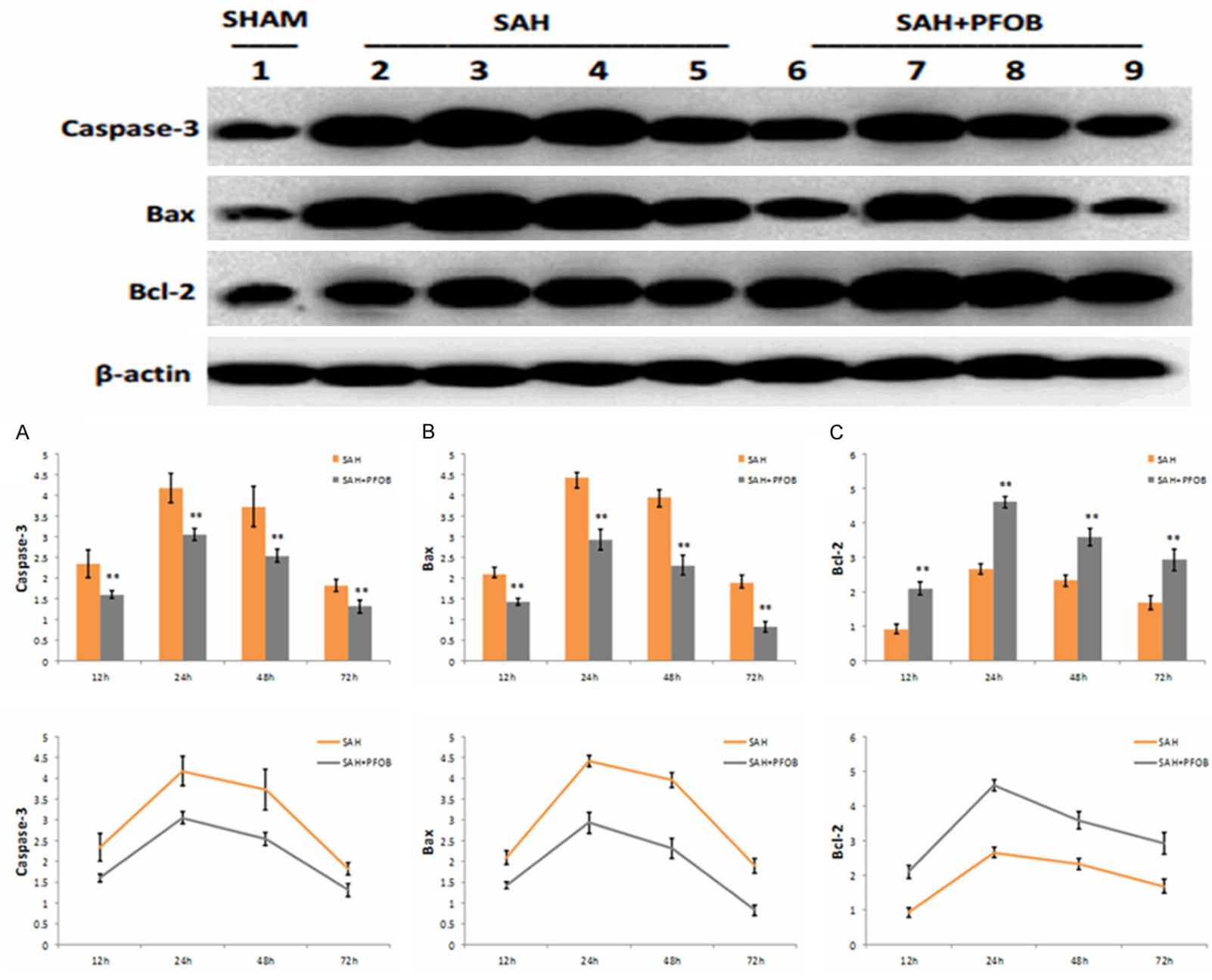
SHAM
SAH
SAH+PFOB
1
2
3
4
5
6
7
8
9
Caspase-3
Bax
Bcl-2
β-actin
A
B
C
SAH
SAH+PFOB
12h
24h
48h
72h

Figure 6. Western blot analysis of caspase-3, Bax, and Bcl-2 protein expression in hippocampal tissues. A-C represent comparison of caspase-3, Bax, and Bcl-2 protein expressions between the SAH and SAH + PFOB groups at 12, 24, 48, and 72 hours postoperatively. 1: the SHAM group; 2-5: the SAH group at 12, 24, 48, and 72 hours postoperatively, respectively; 6-9: the SAH + PFOB group at 12, 24, 48, and 72 hours postoperatively, respectively. β-actin was used as negative control. Data are presented as mean ± SD. **P<0.01 versus SAH group (12 h; 24 h; 48 h; 72 h). N = 5.

enging free radicals [33], preventing hemorrhagic infarction, and reducing the area of hemorrhagic infarction [34].

PFOB belongs to the third generation of PFCs and has higher stability and oxygen carrying capacity than the previous two generations. With smaller particle size, molecules can be distributed more evenly. Also, compound denaturation is unlikely. PFOB can be stored at ambient temperature. Oxygen and carbon dioxide can dissolve in it according to Henry's Law and partial pressure ratio. At one atmosphere under constant temperature, each 100 ml PFOB can dissolve a maximum of about 66 ml of oxygen and about 166 ml of carbon dioxide [9]. Under the same conditions, each 100 ml of blood can dissolve only about 0.3 ml of oxygen, while the oxygen incorporated by hemoglobin is about 18.7 ml, far exceeding that carried by blood. Hence through intravenous injection, PFOB could provide more oxygen to the body. The oxygen molecules in PFOB do not need to cross the red-blood-cell membrane, raising the cellular concentration gradient and making it easier for oxygen molecules to diffuse around the target lesion. Hence, PFOB nanoparticles are safe and stable within organisms, have very high oxygen-carrying ability, good penetrating power and multi-model imaging capability, and can act on lesions rapidly after intravenous injection.

The current study, for the first time, demonstrates that PFOB has a strong protective effect against EBI after SAH. This protective effect was most significant at 24 h after tail vein injection of liquid fluorocarbon nanoparticles. Compared to the SAH group, the PFOB intervention group had significantly reduced brain water content, with alleviated morphological abnormalities in HE-stained neurons and significantly reduced numbers of karyopyknotic or hyperchromatic neurons in the hippocampal CA1 region. Transmission electron microscopy analysis showed that cellular shrinkage, nuclear karyopyknosis, and cytoplasmic hyperchromatism of neurons, as well as swelling and peripheral edema of glial cells after SAH were alleviated to a certain extent. These observations indicate that PFOB can improve the conditions of brain ischemia-hypoxia, posing a protective effect on neurons at cellular and subcellular levels. Western-blot and RT-PCR data showed that expressions of pro-apoptotic factors caspase-3 and bax were significantly reduced, while expression of the anti-apoptotic factor bcl-2 was significantly increased in the corresponding subgroups. Similar results were obtained from TUNEL analysis of neuron apoptosis and immunohistochemical analysis of protein expression in the 24 h SAH subgroup, which exhibited the most significant apoptosis. These results indicated that PFOB exhibited its protective effect on neurons at a molecular level. This preliminary study demonstrates that liquid fluorocarbon nanoparticles dissolved with a high concentration of oxygen can reduce neuronal apoptosis and protect rat neurons, playing a protective role at multiple levels in EBI after SAH. However the exact mechanism through which PFOB plays its protective role is still unclear. We infer that this agent may protect neurons in the following ways: 1) Fluorocarbons have high oxygen uptake-release rates, small particles, and a large concentration gradient of oxygen molecules, thus can rapidly provide brain tissue with adequate oxygen; 2) Fluorocarbons can rapidly remove high concentrations of CO_2 from the microcirculation, thereby mitigating acidosis and relieving vasospasm; fluorocarbons also have low viscosity, thus can dilute red blood cells and fibrinogen, reduce blood viscosity, and improve cerebral blood flow; and 3) fluorocarbons itself doesn't contains any visible component of blood and can reduce the production and release of oxygen free radicals.

Previous studies on PFOB often focus on artificial blood, liquid breathing, multiple angiography contrast agents, and tumor-targeting carriers and so on. This experiment used PFOB in a model of intracranial hemorrhage. Its extremely high oxygen carrying ability and good penetrating power can help to protect neurons from

hypoxic damage in EBI following SAH. Its multimodal imaging capability could also be used to monitor SAH, providing new directions in its treatment. At the same time, most studies on SAH stop at the regulation of neural self-protection. Since the protective effect of self-regulation requires stimulation, signal transduction, transcription control, and protein translation, it is slow and insufficient in the early stages of SAH. In addition, its clinical application still requires long and complicated research. PFOB emulsification has been approved in other countries for the treatment of human coronary angioplasty and acute respiratory distress syndrome. It has good safety and stability in the human body. Through intravenous injection, PFOB emulsification acts on target lesions rapidly and can achieve satisfactory efficacy in a short period of time. The experimental data obtained in this study support the clinical application of PFOB nanoparticles as soon as possible. The next steps still need to be designed and completed to understand the effect of PFOB nanoparticles with high oxygen content in terms of detailed metabolism processes, brain-blood barrier penetration, interaction with neurons, the effects of different doses and so on.

Acknowledgements

This work was supported by funds from Chongqing Natural Science Project Fund (2010JJ0254 to J. Z.), National Clinical Key Specialty Construction Project (to J. Z.), the Bill & Melinda Gates Foundation (to X. W.) and the Muscular Dystrophy Association" (to X. W.).

Disclosure of conflict of interest

None.

Address correspondence to: Dr. Ji Zhu, Department of Neurosurgery, First Affiliated Hospital of Chongqing Medical University, No. 1 Youyi Road, Chongqing 400016, China. Tel: +86 1380-8399-425; Fax: +86 023-6848-5031; E-mail: a68690569@sina.com. Dr. Xin Wang, Department of Neurosurgery, Brigham and Women's Hospital, Harvard Medical School, Boston, Massachusetts, 02115, USA. Tel: +1-617-732-4186; Fax: +1-617-278-6937; E-mail: xwang@rics.bwh.harvard.edu

References

[1] Wang X. Recent advances in stroke: molecular mechanisms, approaches, and treatments. Cent Nerv Syst Agents Med Chem 2011; 11: 80.

[2] Broderick JP, Brott TG, Duldner JE, Tomsick T, Leach A. Initial and recurrent bleeding are the major causes of death following subarachnoid hemorrhage. Stroke 1994; 25: 1342-1347.

[3] Cahill J, Zhang JH. Subarachnoid hemorrhage: is it time for a new direction? Stroke 2009; 40: S86-87.

[4] Cahill J, Calvert JW, Zhang JH. Mechanisms of early brain injury after subarachnoid hemorrhage. J Cereb Blood Flow Metab 2006; 26: 1341-1353.

[5] Kusaka G, Ishikawa M, Nanda A, Granger DN, Zhang JH. Signaling pathways for early brain injury after subarachnoid hemorrhage. J Cereb Blood Flow Metab 2004; 24: 916-925.

[6] Chen J, Chen G, Li J, Qian C, Mo H, Gu C, Yan F, Yan W, Wang L. Melatonin attenuates inflammatory response-induced brain edema in early brain injury following a subarachnoid hemorrhage: a possible role for the regulation of pro-inflammatory cytokines. J Pineal Res 2014; 57: 340-347.

[7] Sehba FA, Hou J, Pluta RM, Zhang JH. The importance of early brain injury after subarachnoid hemorrhage. Prog Neurobiol 2012; 97: 14-37.

[8] Li A, Zheng Y, Yu J, Wang Z. Superparamagnetic perfluorooctyl bromide nanoparticles as a multimodal contrast agent for US, MR, and CT imaging. Acta Radiol 2013; 54: 278-283.

[9] Riess JG. Perfluorocarbon-based oxygen delivery. Artif Cells Blood Substit Immobil Biotechnol 2006; 34: 567-580.

[10] Lacatusu D, Baican M, Crivoi F. Effects of perfluorocarbon emulsion in rheology. Rev Med Chir Soc Med Nat Lasi 2014; 118: 232-238.

[11] Vasquez DM, Ortiz D, Alvarez OA. Hemorheological implications of perfluorocarbon based oxygen carrier interaction with colloid plasma expanders and blood. Biotechnol Prog 2013; 29: 796-807.

[12] Suzuki H, Hasegawa Y, Kanamaru K, Zhang JH. Mechanisms of osteopontin-induced stabilization of blood-brain barrier disruption after subarachnoid hemorrhage in rats. Stroke 2010; 41: 1783-1790.

[13] Song X, Xu R, Xie F, Zhu H, Zhu J, Wang X. Hemin offers neuroprotection through inducing exogenous neuroglobin in focal cerebral hypoxic-ischemia in rats. Int J Clin Exp Pathol 2014; 7: 2163-2171.

[14] Xie F, Xu R, Song X, Zhu H, Wang X, Zhu J. Joint protective effect of exogenous neuroglobin and hemin in rat focal ischemic brain tissues. Int J Clin Exp Med 2014; 7: 2009-2016.

[15] Woods SD, Skinner RD. Progress in dodecafluoropentane emulsion as a neuroprotective agent in a rabbit stroke model. Mol Neurobiol 2013; 48: 363-367.

[16] Zhou Z, Sun D, Levasseur JE. Perfluorocarbon emulsions improve cognitive recovery after lateral fluid percussion brain injury in rats. Neurosurgery 2008; 63: 799-806.
[17] Yacoub A, Hajec MC, Stanger R, Wan W. Neuroprotective effects of perflurocarbon (oxycyte) after contusive spinal cord injury. J Neurotrauma 2014; 31: 256-267.
[18] Edebali N, Tekin IO, Acikgoz B, Acikgoz S, Barut F, Sevinc N, Sumbuloglu V. Apoptosis and necrosis in the circumventricular organs after experimental subarachnoid hemorrhage as detected with annexin V and caspase 3 immunostaining. Neurol Res 2014; 36: 1114-1120.
[19] Hong Y, Shao A, Wang J, Chen S, Wu H. McBride DW, Wu Q, Sun X, Zhang J. Neuroprotective effect of hydrogen-rich saline against neurologic damage and apoptosis in early brain injury following subarachnoid hemorrhage: possible role of the Akt/GSK3β signaling pathway. PLos One 2014; 9: e96212.
[20] Hua F, Cornejo MG, Cardone MH. Effects of Bcl-2 levels on Fas signaling-induced Caspase-3 activation: molecular genetic tests of computational model predictions. J Immunol 2005; 175: 985-995.
[21] Wang X. The antiapoptotic activity of melatonin in neurodegenerative diseases. CNS Neurosci Ther 2009; 15: 345-357.
[22] Wang X. The antiapoptotic effects of melatonin in neonatal hypoxic-ischemic brain injury and adult ischemic stroke. JSM Neurosurgery and Spine 2014; 2: 1033.
[23] Zhou H, Wang J, Jiang J, Stavrovskaya I, Li M, Li W, Wu Q, Zhang X, Luo C, Zhou S, Sirianni AC, Sarkar S, Kristal BS, Friedlander RM, Wang X. N-acetyl-serotonin offers neuroprotection through inhibiting mitochondrial death pathways and autophagic activation in experimental models of ischemic injury. J Neurosci 2014; 34: 2967-2978.
[24] Zhang Y, Wang X, Baranov SV, Zhu S, Huang Z, Fellows-Mayle W, Jiang J, Day AL, Kristal BS, and Friedlander RM. Dipyrone inhibits neuronal cell death and diminishes hypoxic/ischemic brain injury. Neurosurgery 2011; 69: 942-956.
[25] Hasegawa Y, Suzuki H, Sozen T, Altay O, Zhang JH. Apoptotic mechanisms for neuronal cells in early brain injury after subarachnoid hemorrhage. ActaNeuro Chir Suppl 2011; 110: 43-48.
[26] Yuksel S, Tosun YB, Cahill J, Solaroglu I. Early brain injury following aneurysmal subarachnoid hemorrhage: emphasis on cellular apoptosis. Turk Neurosurg 2012; 22: 529-533.
[27] Keipert PE. Perflubron emulsion (Oxygent(tm)): a temporary intravenous oxygen carrier. Anasthesiol Intensivmed Notfallmed Schmerzther 2001; 36 Suppl 2: S104-106.
[28] Clark LC Jr, Gollan F. Survival of mammals breathing organic liquids equilibrated with oxygen at atmospheric pressure. Science 1966; 152: 1755-1756.
[29] Remy B, Deby-Dupont G, Lamy M. Red blood cell substitutes: fluorocarbon emulsions and haemoglobin solutions. Br Med Bull 1999; 55: 277-298.
[30] Spitzer AR, Lipsky CL. Partial 1iquid ventilation with premature infants with severe respiratory distress perflubron in syndrome. Clin Pediatr (Phila) 1997; 36: 181-182.
[31] Lin CY, Javadi M, Belnap DM. Ultrasound sensitive eLiposomes containing doxorubicin for drug targeting therapy. Nanomedicine 2014; 10: 67-76.
[32] Yu YB. Fluorinated dendrimers as imaging agents for ^{19}F MRI. Wiley Interdiscip Rev Nanomed Nanobiotechnol 2013; 5: 646-661.
[33] Rosenblum WI. Fluorocarbon emulsions and cerebral microcirculation. Fed Proc 1975; 34: 1493-1498.
[34] Yokota C, Kaji T, Kuge Y. Temporal and topographic profiles of cyclooxygenase-2 expression during 24 h of focal brain ishemia in rats. Neurosci Lett 2004; 357: 219-222.